Electronic Supplementary Information

Target-activated cascade transcription amplification lights up RNA aptamers for label-free detection of metalloproteinase-2 activity

Ning-ning Zhao,‡[a] Wen-jing Liu,‡[b] Xiaorui Tian,[a] Baogang Zhang,*[c] and Chun-yang Zhang *[a]

[a] College of Chemistry, Chemical Engineering and Materials Science, Shandong Normal University, Jinan 250014, China.

[b] School of Chemistry and Chemical Engineering, Southeast University, Nanjing 211189, China.

[c] Department of Clinical Pathology, Affiliated Hospitcal of Weifang Medical University, Weifang Medical University, Weifang 261053, China.

* Corresponding authors: Tel.: +86 0531-86186033; E-mail: Zhangbg@wfmc.edu.cn; cyzhang@sdnu.edu.cn.

‡ These authors contributed equally.

Experimental section

Chemicals and reagents

All DNA oligonucleotides (Table S1) were synthesized and HPLC purified by Sangon Biotechnology Co. Ltd. (Shanghai, China). The peptides were obtained from the Chinese Peptide Company (Hangzhou, China), and conjugated to DNA by Accurate Biotechnology Co., Ltd. (Hunan, China). Recombinant human MMP-2 protein and recombinant human MMP-7 proteins were purchased from R&D Systems (Minneapolis, MN, USA). The phi29 DNA polymerase, 10× phi29 DNA polymerase reaction buffer (500 mM Tris-HCl, 100 mM $MgCl_2$, 100 mM $(NH_4)_2SO_4$, 40 mM DTT, pH 7.5), T7 RNA polymerase, 10× RNAPol reaction buffer (400 mM Tris-HCl, 60 mM $MgCl_2$, 20 mM spermidine, 100 mM DTT, pH 7.9), uracil-DNA glycosylase (UDG), furin, deoxynucleotide solution mixture (dNTPs), ribonucleotide solution mix (rNTPs), and streptavidin-coated magnetic beads were obtained from New England Biolabs (Ipswich, MA, USA). Caspase-8 (human, recombinant, active) and caspase-9 (human, recombinant, active) were obtained from Enzo Biochem, Inc. (Farmingdale, NY, USA). BB-2516 were purchased from Sigma-Aldrich Company (St. Louis, MO, U.S.A.). SYBR Gold was obtained from Invitrogen Co. (Carlsbad, CA, USA). Human cervical carcinoma cell line (HeLa cells), human breast cancer cell line (MDA-MB-231 cells and MCF-7 cells), human colorectal carcinoma cell line (HCT-116 cells), normal human liver cell line (LO2 cells), and human embryonic kidney cell line (HEK 293 cells) were purchased from Cell Bank of Chinese Academy of Sciences (Shanghai, China). Nuclear extract kit was brought from Active Motif (Carlsbad, CA, USA). Human MMP-2 ELISA Kit and DEPC-treated water were obtained from Sangon Biotechnology Co. Ltd. (Shanghai, China). The ultrapure water was prepared by a Millipore filtration system (Millipore, Milford, MA, USA).

Table S1. Sequence of synthesized oligonucleotides [α]

Note	Sequence (5′-3′)
Conjugate probe	Biotin-(COOH)-KKGRV-GLPGC-(NH_2)-TGA GGT AGT AGG TTG TAT AGT T
Circular template	**CTA CTA CCT CA**G GGA GCT CAC ACT CTA CTC AAC AGC GCG AAC GCT GGA CCC GTC CTT CTC CCG CCC TAT AGT GAG TCG TAT TA**A ACT ATA CAA C**
Primer	AAC TAT ACA ACC TAC TAC CTC A

[α] In the circular template, the bold indicates the hybridization region for DNA trigger.

Assembly of the conjugate probes with the streptavidin-coated magnetic beads

The 100 μL of 10 mg/mL streptavidin-coated MBs solution was washed twice with 1× PBS. After resuspending in 1× PBS, 500 nM conjugate probe was added to form the conjugate probe-MB nanostructure through biotin-streptavidin interaction at room temperature for 30 min. The resultant nanostructures were then washed five times with 1× PBS to remove the uncoupled probes by magnetic separation.

MMP-2-mediated cleavage of conjugate probes

The MMP-2-mediated cleavage of conjugate probes was performed in 10 μL of solution containing different concentrations of MMP-2, 2 μL of conjugate probe-MB nanostructure, 1 × TCNB buffer (50.0 mM Tris-HCl, 10.0 mM $CaCl_2$, 150 mM NaCl, 0.05% Brij-35, pH 7.5), and incubated at 37 ℃ for 2 h. After magnetic separation, the supernatant with cleavage products was collected for further use.

Hyperbranched rolling circle amplification

Hyperbranched rolling circle amplification (HRCA) was performed in 20 μL of reaction solution

containing 2 μL of supernatant solution, 1 nM circular template, 50 nM primer, 30 μM dNTPs, 4 U of phi29 DNA polymerase, and 1× phi29 DNA polymerase reaction buffer (50 mM Tris-HCl, 10 mM $MgCl_2$, 10 mM $(NH_4)_2SO_4$, 4 mM DTT, pH 7.5), and incubated at 30 °C for 1 h, followed by inactivation at 65 °C for 10 min.

Transcription amplification

The transcription amplification was carried out in 30 μL of solution containing 20 μL of the HRCA products, 500 μM rNTPs, 30 U of T7 RNA polymerase, and 1× RNAPol reaction buffer (40 mM Tris-HCl, 6 mM $MgCl_2$, 2 mM spermidine, 10 mM DTT, pH 7.9), and incubated at 37 °C for 60 min. Then, 30 μL of transcription products and 10 μM DFHBI were incubated for 3 min at room temperature.

Fluorescence measurement and gel electrophoresis

Fluorescence emission spectra were obtained using an F-1000 fluorescence spectrophotometer (Edinburgh Instruments, UK) with 468-nm excitation. The emission spectra from 480 to 600 nm were recorded with both emission and excitation slits of 2 nm. Data analysis was performed using the fluorescence intensity at 504 nm. The MMP-2 cleavage products were analyzed using 12% native polyacrylamide gel electrophoresis (PAGE) in 1 × TBE buffer (49.5 mM Tris-HCl, 49.5 mM boric acid, 2.0 mM EDTA, pH 8.0) at 110 V for 65 min. The HRCA products and transcription products were analyzed by 2% agarose gel electrophoresis in 1× TAE buffer (40 mM Tris-acetic acid, 1 mM EDTA, pH 8.0) at 110 V for 70 min. After staining with SYBR Gold, the gel was imaged using Bio-Rad ChemiDoc MP imaging system (California, U.S.A.).

Kinetic analysis

To evaluate the enzyme kinetic parameters of MMP-2, we measured the initial velocity in the presence

of 10 nM MMP-2 and different-concentration conjugate probe in 5-min reaction at 37 °C. The kinetic parameters are fitted to the Michaelis-Menten equation.

$$V = \frac{V_{max} + [S]}{K_m + [S]}$$

where V_{max} is the maximum initial velocity, and [S] is the concentration of conjugate probe, and K_m is the Michaelis-Menten constant.

Inhibition assay

Different-concentration BB-2516 was incubated with 10 nM MMP-2, 2 μL of conjugate probe-MB nanostructure, 1 × TCNB buffer (50.0 mM Tris-HCl, 10.0 mM $CaCl_2$, 150 mM NaCl, 0.05% Brij-35, pH 7.5) at 37 °C for 2 h. The relative activity (RA) of MMP-2 is determined according to equation 1.

$$RA\ (\%) = \frac{C_i}{C_t} \times 100\% = 10^{(F_i - F_t)/1768.77} \times 100\% \qquad (1)$$

Where F_t represents the fluorescence intensity generated by MMP-2, and F_i represents the fluorescence intensity generated by MMP-2 and BB-2516. C_t and C_i were obtained according to linear equation in inset of Fig. 2A. The IC_{50} value was obtained from the inhibition curve.

Cell culture and preparation of cell extracts

Human cervical carcinoma cell line (HeLa cells), human breast cancer cell line (MDA-MB-231 cells and MCF-7 cells), normal human liver cell line (LO2 cells) and human embryonic kidney cell line (HEK 293 cells) were cultured in Dulbecco's modified Eagle's medium (DMEM, Invitrogen, USA) supplemented with 10 % fetal bovine serum and 1% penicillin-streptomycin in 5% CO_2 incubator at 37 ℃. Human colorectal carcinoma cell line (HCT-116 cells) was cultured in McCoy's 5A medium (Gibco, USA) supplemented with 10 % fetal bovine serum and 1% penicillin-streptomycin. The cell lysates were prepared by using a nuclear extract kit (Active Motif, Carlsbad, CA, USA). The resultant cell extracts were used for MMP-2 assay immediately.

Determination of MMP-2 in serum samples

Human serum samples were diluted to ensure that the MMP-2 concentrations were in the linear range. Then the appropriate aliquots of serum samples were added to the reaction mixture, and MMP-2 in the diluted serum samples was quantified according to the procedure described above.

ELISA analysis

The concentration of MMP-2 in serum samples was measured by using a human MMP-2 enzyme-linked immunosorbent assay (ELISA) kit (Sangon Biotech Co., Ltd., Shanghai, China). The optical densities (ODs) were quantified by a SpectraMax i3 multimode microplate reader (Molecular Devices, San Jose, CA, USA) at a wavelength of 450 nm.

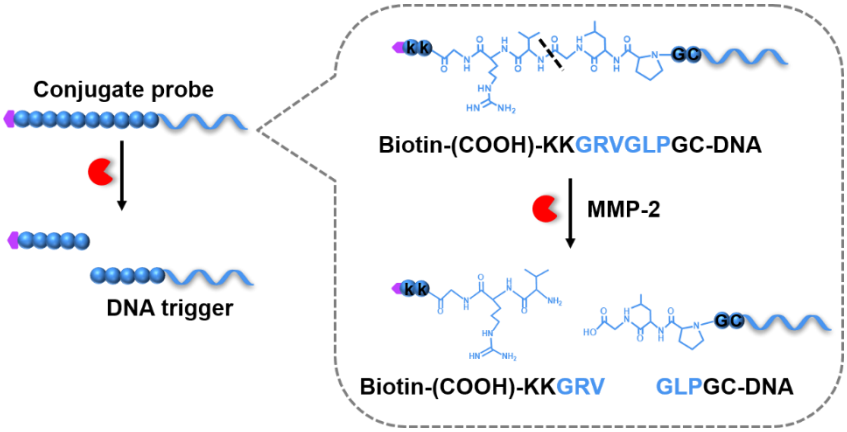

Fig. S1 Chemical structure and cleavage process of the peptide-DNA conjugate probe.

Optimization of experimental conditions

To achieve the best assay performance, we optimized a series of experimental parameters including the concentration of primer, the amount of dNTP, the HRCA time, the concentrations of phi29 DNA polymerase and T7 RNA polymerase, and the amount of rNTP. We investigated the influence of experimental parameters upon the F/F_0 value, where F and F_0 are the fluorescence intensity in the

presence and absence of target MMP-2, respectively.

The concentration of primer may affect the amplification efficiency of HRCA. On one hand, high-concentration primer induces high amplification efficiency, but it might increase the background correspondingly. On the other hand, low-concentration primer decreases the background, but it may induce low amplification efficiency. We monitored the variance of the F/F_0 value with different concentrations of primer. As shown in Fig. S2A, a maximum F/F_0 value is obtained at the primer concentration of 50 nM. Thus, 50 nM primer is selected for MMP-2 assay in the following research.

We further investigated the effect of the dNTP concentration upon the amplification efficiency of HRCA. As shown in Fig. S2B, the F/F_0 value enhances with the increasing concentration of dNTP from 10 to 30 μM, follow by the decrease beyond the concentration of 30 μM. Thus, 30 μM dNTP is selected for MMP-2 assay in the following research.

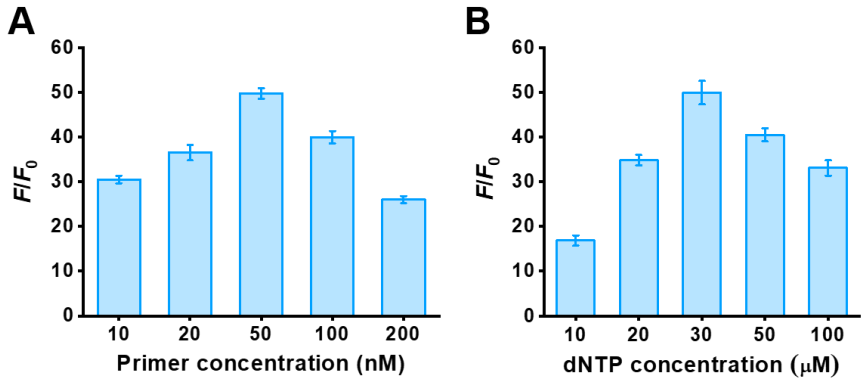

Fig. S2 (A) Variance of the F/F_0 value with the concentration of primer. (B) Variance of the F/F_0 value with the concentration of dNTP. The MMP-2 concentration is 10 nM. Data represented means ± SD, n = 3.

The reaction time of HRCA is the essential element that determines the yield of transcription templates and promoters. We investigated the effect of the HRCA time upon the assay performance. As

shown in Fig. S3A, the F/F_0 value enhances with the HRCA time from 10 to 60 min, and reaches the plateau at 60 min. Thus, 60 min of HRCA time is selected for MMP-2 assay in the following research. Moreover, the amplification efficiency of HRCA relies on phi29 DNA polymerase. The concentration of phi29 DNA polymerase should be optimized. We investigated the influence of phi29 DNA polymerase upon the amplification efficiency. As shown in Fig. S3B, the F/F_0 value enhances with the increasing amount of phi29 DNA polymerase from 1 to 4 U, and levels off beyond 4 U. Thus, 4 U of phi29 DNA polymerase is selected for MMP-2 assay in the following research.

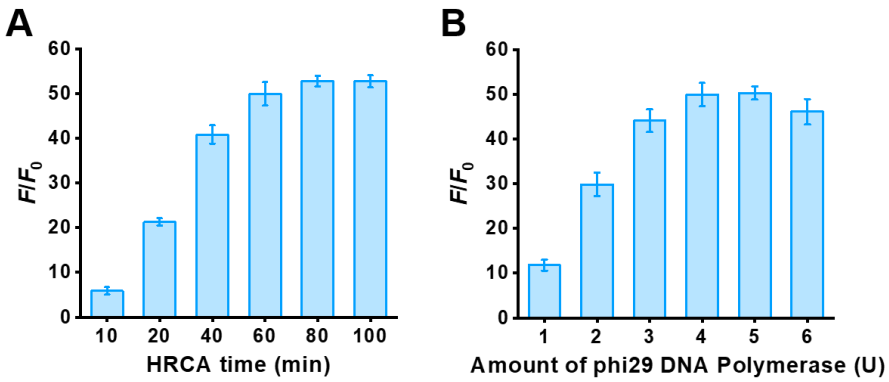

Fig. S3 (A) Variance of the F/F_0 value with the HRCA time. (B) Variance of the F/F_0 value with the amount of phi29 DNA polymerase. The MMP-2 concentration is 10 nM. Data represented means ± SD, n = 3.

In this assay, the amplification efficiency of transcription reaction relies on the amount of T7 RNA polymerase and the concentration of rNTP. Therefore, the amount of T7 RNA polymerase and the concentration of rNTP should be carefully optimized. As shown in Fig. S4A, the F/F_0 value enhances with the increasing amount of T7 RNA polymerase from 10 to 30 U, followed by the decrease beyond the amount of 30 U. Thus, 30 U of T7 RNA polymerase is selected for MMP-2 assay in the following research.

We further studied the effect of rNTP upon the amplification efficiency of transcription reaction. As shown in Fig. S4B, the F/F_0 value enhances with the increasing concentration of rNTP from 100 to 500 μM, and reaches the maximum value at the concentration of 500 μM. Thus, 500 μM rNTP is selected for MMP-2 assay in the following research.

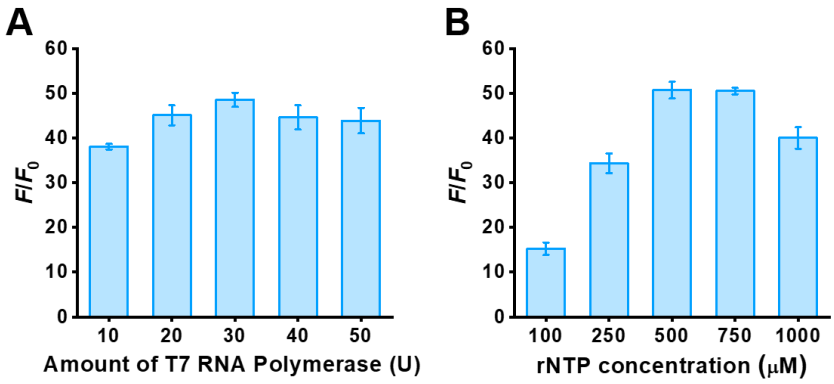

Fig. S4 (A) Variance of the F/F_0 value with different amount of T7 RNA polymerase (B) Variance of the F/F_0 value with different concentration of rNTP. The MMP-2 concentration is 10 nM. Data represented means ± SD, n = 3.

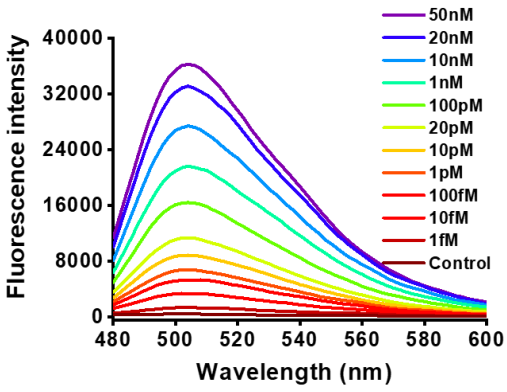

Fig. S5 Fluorescence emission spectra in response to different concentrations of MMP-2.

Detection selectivity

To evaluate the slectivity of this assay, we introduced matrix metalloproteinase-7 (MMP-7), caspase-9, bovine serum albumin (BSA), uracil DNA glycosylase (UDG), protein kinases (PKA), and furin as the interferences. MMP-7 is a protease homologous to MMP-2.[1] Caspase-9 is a kind of cysteinyl aspartate-directed proteases with the capability of cleaving the tetrapeptide sequence Leu-Glu-His-Asp.[2] BSA is a commonly irrelevant protein.[3] UDG can catalyze the excision of the damaged uracil base from both single-stranded and double-stranded DNA.[4] PKA can catalyze the phosphorylation of substrate peptide.[5] Furin can specifically cleave short peptide sequences.[6] As depicted in Fig. 2B, only MMP-2 can generate a high fluorescence signal (Fig. 2B, red column), which is much higher than those generated by MMP-7 (Fig. 2B, blue column), caspase-9 (Fig. 2B, purple column), BSA (Fig. 2B, yellow column), UDG (Fig. 2B, pink column), PKA (Fig. 2B, cyan column), furin (Fig. 2B, orange column), and control group (Fig. 2B, grey column). Moreover, a high fluorescence signal is generated by adding 10 nM MMP-2 into the interferences (Fig. 2B, green column), which is identical to that generated by 10 nM MMP-2 alone (Fig. 2B, red column), indicating good selectivity and anti-interferences capability of the proposed assay.

Kinetic analysis

We employed this assay to measure the kinetic parameters. The initial velocities (V) are determined in the presence of 10 nM MMP-2 and different concentrations of conjugate probe from 0 to 10 μM in 5-min reaction at 37 °C. As depicted in Fig. 2C, the initial velocity (V) of MMP-2 gradually enhances with the increasing concentration of conjugate probe. Kinetic parameters are measured according to the Michaelis-Menten equation $V = V_{max}[S]/(K_m + [S])$, where V_{max} is the maximum initial

velocity, [*S*] is the concentration of conjugate probe, and K_m is the Michaelis-Menten constant. The V_{max} and K_m are determined to be 28263.02 min^{-1} and 1.15 μM, respectively. The K_m is consistent with that measured by single-molecule detection (K_m = 1.24 μM),[1] indicating that this assay can analysis the kinetic parameters of MMP-2.

Detection of MMP-2 activity in different cell lines

We measured the MMP-2 activity in four cancer cell lines including human colorectal carcinoma cell line (HCT-116 cells), human breast cancer cell line (MDA-MB-231 cells and MCF-7 cells), and human cervical carcinoma cell line (HeLa cells), and two normal cell lines including normal human liver cell line (LO2 cells) and human embryonic kidney cell line (HEK 293 cells). As depicted in Fig. 3A, no distinct fluorescence signals are produced by HEK 293 cells (Fig. 3A, pink column) and LO2 cells (Fig. 3A, green column), with no significant difference from the zero background signal generated by the control group without cell extracts (Fig. 3A, grey column), indicating the ultralow expression level of MMP-2 in normal cells.[7] In contrast, distinct fluorescence signals are detected in HCT-116 cells (Fig. 3A, red column), MDA-MB-231 cells (Fig. 3A, blue column), MCF-7 cells (Fig. 3A, purple column), and HeLa cells (Fig. 3A, orange column). Especially, the fluorescence signals produced by HCT-116 cells and MDA-MB-231 cells are much higher than that produced by MCF-7 cells and HeLa cells, suggesting that high overexpression level of MMP-2 in high malignant cells than those in low malignant cells.[8]

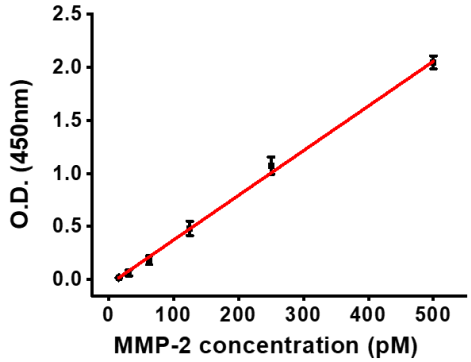

Fig. S6 Linear relationship between the optical density (O.D.) and the MMP-2 concentration. Data represented means ± SD, n = 3.

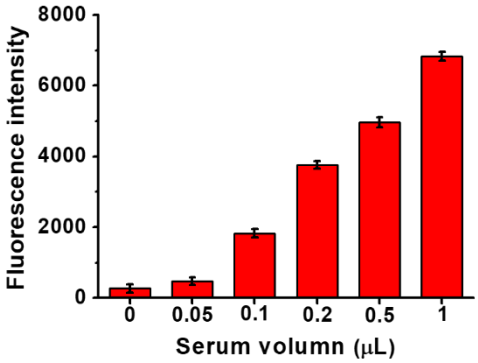

Fig. S7 Measurement of fluorescence intensity in response to serum volume from 0 to 1 μL. Data represented means ± SD, n = 3.

Table S2. Comparison of the proposed assay with the reported methods for MMP-2 detection [α]

Method	Signal model	Assay time	LOD (M)	Linear range (M)	Real samples	Ref.
Magnetic resonance imaging (MRI)	T_1-weighted MRI phantoms	>12 h	5×10^{-10}	/	live cells	9
Quantum dots- based fluorescence assay	Fluorescence	>12 h	2.5×10^{-10}	$0 – 2 \times 10^{-9}$	live cells mice	10
Graphene oxide-peptide based fluorescence sensor	Fluorescence	4.5 h	5×10^{-11}	$2 \times 10^{-10} – 2 \times 10^{-9}$	live cells	11
Ratiometric NIR Fluorescent Nanoprobe	Fluorescence	>12 h	3.6×10^{-11}	$5 \times 10^{-11} – 1 \times 10^{-9}$	live cells mice	12
Poly(m-phenylenediamine)-based fluorescent nanoprobe	Fluorescence	12 h	3.2×10^{-11}	1×10^{-10}–2×10^{-8}	live cells serum samples	13
Protease sensor based on protease-sensitive cleavage and nicking enzyme-assisted signal amplification	Fluorescence	5 h	3.33×10^{-12}	3.8×10^{-12}– 1.2×10^{-9}	live cells	1
One-step sandwich assay based on surface plasmon resonance	Resonance units	1 h	5×10^{-13}	$0 – 5 \times 10^{-12}$	No	14
Silicon nanowire-based biosensor	Conductance	7 h	1×10^{-13}	1×10^{-13}– 1×10^{-8}	No	15
Target-activated transcription-based fluorescence assay	Fluorescence	40 min	7×10^{-14}	$3 \times 10^{-13} –7 \times 10^{-9}$	live cells tissue samples	16
Label-free electrochemical biosensor	Current	>12 h	7.1×10^{-15}	$1 \times 10^{-14} – 1 \times 10^{-9}$	live cells tissue samples	17
Fluorescence assay based on cascade transcription amplification	Fluorescence	4.5 h	6×10^{-16}	$1 \times 10^{-15} – 1 \times 10^{-11}$	live cells serum samples	This work

[α] Assay time includes preparation time and MMP-2 detection time.

Table S3. Recovery ratios of MMP-2 in 1000-fold diluted human serum

Serum	Initial (diluted) (pM)	Added (pM)	Detected (pM)	Recovery (%)	RSD (%)
1	1.49	2	3.44	98.57	1.15
2	1	2	2.68	101.69	1.33
3	1.73	2	3.61	96.78	2.18
4	2.48	5	7.77	103.88	2.75
5	1.27	5	6.35	101.28	0.95
6	1.82	5	7.19	104.05	2.84

References

1 Y. Y. Li, W. Liu, Q. F. Xu, J. Hu and C. Y. Zhang, *Biosens. Bioelectron.*, 2020, **169**.

2 M. Liu, R. Xu, W. Liu, J. G. Qiu, Y. Wang, F. Ma and C. Y. Zhang, *Chem Sci*, 2021, **12**, 15645-15654.

3 F. Ma, Y. Yang and C. Y. Zhang, *Anal. Chem.*, 2014, **86**, 6006-6011.

4 B. R. Li, H. Tang, R. Q. Yu and J. H. Jiang, *Anal. Chem.*, 2021, **93**, 8381-8385.

5 S. Martic, M. Gabriel, J. P. Turowec, D. W. Litchfield and H. B. Kraatz, *J. Am. Chem. Soc.*, 2012, **134**, 17036-17045.

6 J. J. Hu, W. L. Jiang, Q. Chen, R. Liu, X. D. Lou and F. Xia, *Anal. Chem.*, 2021, **93**, 14036-14041.

7 Y. P. Wang, T. T. Lin, W. Y. Zhang, Y. F. Jiang, H. Y. Jin, H. N. He, V. C. Yang, Y. Chen and Y. Z. Huang, *Theranostics*, 2015, **5**, 787-795.

8 (a) Z. Lei, H. Zhang, Y. Q. Wang, X. Y. Meng and Z. X. Wang, *Anal. Chem.*, 2017, **89**, 6749-6757;

(b) L. Wang, H. Li, L. Shi, L. Li, F. J. Jia, T. Gao and G. X. Li, *Biosens. Bioelectron.*, 2022, **195**; (c) Y. Wang, T. Lin, W. Zhang, Y. Jiang, H. Jin, H. He, V. C. Yang, Y. Chen and Y. Huang, *Theranostics*, 2015, **5**, 787-795.

9 X. Zhu, H. Lin, L. Wang, X. Tang, L. Ma, Z. Chen and J. Gao, *ACS Appl Mater Interfaces*, 2017, **9**, 21688-21696.

10 X. Li, D. Deng, J. Xue, L. Qu, S. Achilefu and Y. Gu, *Biosens. Bioelectron.*, 2014, **61**, 512-518.

11 D. Feng, Y. Zhang, T. Feng, W. Shi, X. Li and H. Ma, *Chem. Commun.* , 2011, **47**, 10680-10682.

12 W. Zeng, L. Wu, Y. Sun, Y. Wang, J. Wang and D. Ye, *Small*, 2021, **17**, e2101924.

13 Z. Wang, X. Li, D. Feng, L. Li, W. Shi and H. Ma, *Anal. Chem.*, 2014, **86**, 7719-7725.

14 U. Pieper-Furst, U. Kleuser, W. F. Stocklein, A. Warsinke and F. W. Scheller, *Anal. Biochem.*, 2004, **332**, 160-167.

15 J. H. Choi, H. Kim, J. H. Choi, J. W. Choi and B. K. Oh, *ACS Appl Mater Interfaces*, 2013, **5**, 12023-12028.

16 F. Liu, M. Yang, W. Song, X. Luo, R. Tang, Z. Duan, W. Kang, S. Xie, Q. Liu, C. Lei, Y. Huang, Z. Nie and S. Yao, *Chem Sci*, 2020, **11**, 2993-2998.

17 K. Shi, L. Cao, F. Liu, S. Xie, S. Wang, Y. Huang, C. Lei and Z. Nie, *Biosens. Bioelectron.*, 2021, **190**, 113372.